

# Advanced Compact Model for the Charges and Capacitances of Short-Channel MOS Transistors

Oscar da Costa Gouveia-Filho<sup>1,2</sup>, Márcio Cherem Schneider<sup>1</sup> and Carlos Galup-Montoro<sup>1</sup>

1. Laboratório de Circuitos Integrados (LCI) - Departamento de Engenharia Elétrica - UFSC  
C.P. 476 - CEP 88040-900 Florianópolis - SC - Brasil
2. Centro de Instrumentação Eletrônica (CIEL) - Departamento de Engenharia Elétrica - UFPR -  
C.P. 19011 - CEP - 81531-970 Curitiba - PR - Brasil  
E-mail: [ogouveia@eletr.ufpr.br](mailto:ogouveia@eletr.ufpr.br)

## Abstract

*This paper presents a new compact model for the intrinsic charges and (trans)capacitances of the MOSFET including short-channel effects such as drain induced barrier lowering (DIBL), channel length modulation (CLM) and carrier velocity saturation. Explicit and compact expressions for charges and (trans)capacitances valid in all regimes of operation are presented. Simulations examples that illustrate short-channel effects in charges and (trans)capacitances are shown.*

## 1. Introduction

In the last years, many efforts have been made to improve the modeling of the dc characteristics of small-geometry MOSFET's. However, the design of analog-digital circuits for low voltage operation at high-speed requires the ac characteristics to be accurately modeled as well.

Some recent models present expressions for the intrinsic charges. The models in [1-2] show explicit and continuous expressions for the charges but do not take into account velocity saturation. BSIM model [3] uses very complicated expressions for the charges with many fitting parameters, is discontinuous for  $V_{DS}=0$  and does not keep the source-drain symmetry of the MOSFET

In this paper we present a new model for the intrinsic charges and (trans)capacitances which rests on the short-channel charge model of Maher [4] and the model presented in [1]. The new model keeps transistor symmetry, has consistent expressions for the charges and (trans)capacitances, is continuous around  $V_{DS}=0$ , and includes the effects of charge sharing, DIBL, CLM and velocity saturation.

## 2. Basic Relations

The equations that follows have been derived for NMOS transistors. The basic assumption of this model is the linear dependence of the inversion charge density  $Q'_i$  on the surface potential  $\phi_s$ , for a given gate-to-bulk voltage ( $V_G$ ).

The short channel effects are included in the model as described in [1]. The DIBL effect is represented by the parameter  $\sigma$ , which models the dependence of the pinch-off voltage,  $V_p$ , on both the drain and source voltages according to:

$$V_p(V_G, V_S, V_D) = V_{p0}(V_G) + \frac{\sigma}{n}(V_D + V_S) \quad (1)$$

where  $V_G$ ,  $V_S$ , and  $V_D$  are the gate, source and drain voltages referred to the substrate, respectively.  $V_{p0}(V_G)$  is the pinch-off voltage for  $V_D=V_S=0$ . The CLM is represented by a shrinkage of the channel length  $\Delta L$  given by a conventional expression [1].

The effect of carrier velocity saturation is included in the mobility model as [1, 4]

$$\mu_s = \frac{\mu}{1 + \frac{\mu}{v_{lim}} \frac{d\phi_s}{dx}} \quad (2)$$

where  $v_{lim}$  is the saturation velocity and  $\mu$  is the mobility of the long-channel device, which has been assumed to be a function of  $V_G$  only.

The drain current including velocity saturation is given by

$$I_D = \frac{\mu W_{eff}}{C'_{ox} L_{eq}} \frac{1}{1 + \frac{Q'_R - Q'_F}{Q'_A}} \frac{Q'_F{}^2 - Q'_R{}^2}{2n} \quad (3)$$

where  $L_{eff}$  and  $W_{eff}$  are the effective channel length and width,  $Q'_{F(R)} = Q'_{IS(D)} - nC'_{OX}\phi_t$ ,  $L_{eq} = L_{eff} - \Delta L$  and

$Q'_A = nC'_{ox} L_{eq} \frac{v_{lim}}{\mu}$ .  $Q'_{IS(D)}$  is the inversion charge density

evaluated at the source (drain) end.  $C'_{ox}$  is the gate capacitance per unit area,  $\phi_t$  is the thermal voltage and  $n$  the slope factor.

The relationship between the inversion charge and the terminal voltages used is the so called unified charge control model (UCCM) [1, 5].

### 3. Intrinsic Charges

The inversion and depletion charges are given by

$$Q_I = W_{eff} \int_0^{L_{eff}} Q'_I dx, \quad Q_B = W_{eff} \int_0^{L_{eff}} Q'_B dx. \quad (4-5)$$

respectively.  $dx$  can be written as

$$dx = -\frac{\mu W_{eff}}{nC'_{ox} I_D} \left( Q'_I - nC'_{ox} \phi_t + \frac{I_D}{W_{eff} v_{lim}} \right) dQ'_I. \quad (6)$$

To calculate the total inversion charge, the channel is split into the saturated and nonsaturated regions. Substituting (3) and (6) into (4) and integrating from  $L = 0$  to  $L = L_{eq}$  we obtain the inversion charge in the nonsaturated region of the channel. In the saturated region the inversion charge density is considered to be constant and therefore, the inversion charge is equal to  $W_{eff} \Delta L Q'_{ID}$ .

Thus, the total inversion charge is

$$Q_I = W_{eff} L_{eq} \left( \frac{2q_r^2 + q_r q_f + q_f^2}{3(q_f + q_r)} + nC'_{ox} \phi_t - \frac{I_D}{W_{eff} v_{lim}} \right) + W_{eff} \Delta L Q'_{ID} \quad (7)$$

where

$$q_r = Q'_F + \frac{I_D}{W_{eff} v_{lim}} \quad (8a)$$

and

$$q_f = Q'_R + \frac{I_D}{W_{eff} v_{lim}}. \quad (8b)$$

The depletion charge density is given by

$$Q'_B = -\frac{n-1}{n} Q'_I - \frac{\gamma^2 C'_{ox}}{2(n-1)} \quad (9)$$

which after integration along the channel gives

$$Q_B = -\frac{n-1}{n} Q_I - W_{eff} L_{eq} \frac{\gamma^2 C'_{ox}}{2(n-1)}. \quad (10)$$

The gate charge is given by

$$Q_G = -Q_B - Q_I = -\frac{Q_I}{n} + W_{eff} L_{eq} \frac{\gamma^2 C'_{ox}}{2(n-1)}. \quad (11)$$

The drain charge is given by

$$Q_D = W_{eff} \int_0^{L_{eq}} \frac{x}{L} Q'_I dx + W_{eff} \int_{L_{eq}}^{L_{eff}} Q'_{ID} dx \quad (12)$$

where we integrate along the saturated and nonsaturated regions of the channel. The coordinate  $x$  is obtained by

integrating (6) from the source ( $x = 0, Q'_I = Q'_{IS}$ ) to an arbitrary point of the channel ( $x, Q'_I$ ):

$$x = \frac{\mu W_{eff}}{2nC'_{ox} I_D} \left[ \left( Q'_{IS} - nC'_{ox} \phi_t + \frac{I_D}{W_{eff} v_{lim}} \right)^2 - \left( Q'_I - nC'_{ox} \phi_t + \frac{I_D}{W_{eff} v_{lim}} \right)^2 \right] \quad (13)$$

Substituting (13) in (12) and integrating we obtain

$$Q_D = \frac{W_{eff} L_{eq}^2}{L_{eff}} \left( \frac{2}{15} \frac{3q_r^3 + 6q_r^2 q_f + 4q_r q_f^2 + 2q_f^3}{(q_f + q_r)^2} + \frac{nC'_{ox} \phi_t - \frac{I_D}{W_{eff} v_{lim}}}{2} + W_{eff} \frac{L_{eff}^2 - L_{eq}^2}{2L_{eff}} Q'_{ID} \right) \quad (14)$$

Finally the source charge is

$$Q_S = Q_I - Q_D. \quad (15)$$

Note that equations (10) and (14) have the same form of their counterparts in the long channel model reported in [1], as long as CLM is not accounted for.

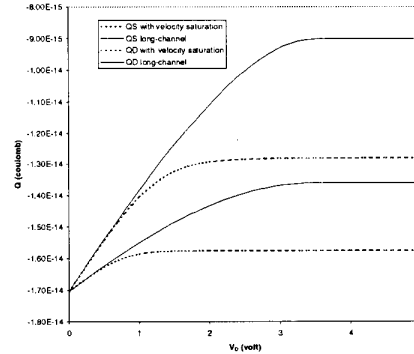


**Fig. 1 - Source and drain charges versus  $V_D$  for the model with velocity saturation and for the long-channel model.**

The effect of velocity saturation is an increase in the absolute value of the total inversion charge in saturation as a consequence of the non zero charge density at the drain end. This effect is illustrated in Fig. 1 where the source and drain charges are plotted together with the charges obtained from the long channel model of [1]. The difference between the long-channel and short channel characteristics can be viewed as a reduction of the saturation voltage due to  $v_{lim}$ . In Fig. 2 the effects of both CLM and DIBL are shown. DIBL causes an increase in the absolute value of the charges, in the saturation region, as predicted by equation (1). In saturation DIBL combined with velocity saturation can produce a maximum in the charge characteristics, as shown in Fig. 2.

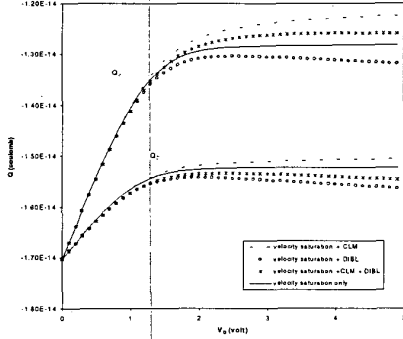


Fig.2 - Drain and source charges showing the effects of CLM and DIBL separately and combined with one another.

#### 4. Transcapacitances

The (trans)capacitances are defined as

$$C_{kj} = -\frac{\partial Q_k}{\partial V_j}, \quad C_{ji} = \frac{\partial Q_j}{\partial V_i} \quad (16)$$

where  $Q_k$  and  $Q_j$  are any of the charges  $Q_G$ ,  $Q_B$ ,  $Q_S$  or  $Q_D$  and  $V_j$  is any of the potentials  $V_G$ ,  $V_B$ ,  $V_S$  or  $V_D$ . The expressions above define 16 (trans)capacitances from which we can choose 9 that are independent.

Applying the definition (16) and using (11) the gate to source ( $C_{gs}$ ) and gate to drain ( $C_{gd}$ ) capacitances are written as

$$C_{gs(d)} = \frac{\partial Q_G}{\partial V_{S(D)}} = \frac{1}{n} \frac{\partial Q_I}{\partial V_{S(D)}} \quad (17)$$

From (7) we have

$$\frac{\partial Q_I}{\partial V_{S(D)}} = \frac{\partial Q_I}{\partial q_f} \frac{\partial q_f}{\partial V_{S(D)}} + \frac{\partial Q_I}{\partial q_r} \frac{\partial q_r}{\partial V_{S(D)}} - \frac{L_{eq}}{v_{lim}} \frac{\partial I_D}{\partial V_{S(D)}} \quad (18)$$

Considering that the partial derivatives of the drain current with respect to the source and drain voltages define the source and drain transconductances ( $g_{ms}$  and  $g_{md}$ ) respectively we have,

$$\frac{\partial q_{f(r)}}{\partial V_{S(D)}} = nC'_{ox} \left( 1 + \frac{nC'_{ox}\phi_t}{Q'_{F(R)}} \right) \left( 1 + \frac{\sigma}{n} \right) + \frac{g_{ms(d)}}{W_{eff} v_{lim}} \quad (19)$$

$$\frac{\partial q_{f(r)}}{\partial V_{D(S)}} = -nC'_{ox} \left( 1 + \frac{nC'_{ox}\phi_t}{Q'_{F(R)}} \right) \frac{\sigma}{n} + \frac{g_{md(s)}}{W_{eff} v_{lim}} \quad (20)$$

In (19) and (20) the partial derivatives of  $\Delta L$  have been neglected.

Here we define

$$C'_{gs(d)o} = C'_{ox} \left( 1 + \frac{nC'_{ox}\phi_t}{Q'_{F(R)}} \right) \frac{\partial Q_I}{\partial q_{f(r)}} \quad (21)$$

We have chosen this notation because  $C_{gs0}$  and  $C_{gd0}$  are exactly the long channel capacitances  $C_{gs}$  and  $C_{gd}$  reported in [1].

Proceeding the same way, the expressions for (trans)capacitances  $C_{gb}$ ,  $C_{dd}$ ,  $C_{ds}$ ,  $C_{dg}$  and  $C_{db}$ , are found. The expressions for the capacitances are listed in table 1. In those expressions  $g_{mb}$  and  $g_{mg}$  are, respectively the bulk and gate transconductances.  $C_{dd0}$  and  $C_{dso}$ , the values of  $C_{dd}$  and  $C_{ds}$  if short-channel effects are not account for, are:

$$C_{dd0} = nC'_{ox} \left( 1 + \frac{nC'_{ox}\phi_t}{Q'_R} \right) \frac{\partial Q_D}{\partial q_f} \quad (22)$$

$$C_{dso} = nC'_{ox} \left( 1 + \frac{nC'_{ox}\phi_t}{Q'_F} \right) \frac{\partial Q_D}{\partial q_r} \quad (23)$$

Fig. 3 shows  $C_{gs}$  and  $C_{gd}$ , normalized to the gate capacitance  $C_{ox}$ , versus  $V_D$ , calculated according to the expressions of Table 1. The long-channel capacitances, denoted by  $C_{kjo}$ , can be calculated from the long-channel model described in [1]. These capacitances vary more abruptly when we include velocity saturation than in the long channel model. This result is coherent with the smaller  $V_{DSAT}$  obtained when velocity saturation is considered

Fig. 4 shows the dependence of  $C_{gd}$ , and  $C_{gs}$  on the channel length. Due to DIBL  $C_{gd}$  becomes negative for the transistor whose channel length is  $0.8\mu m$ , the minimum value for this technology. Finally, Fig. 5 shows these same transcapacitances and the gate capacitance versus  $V_G$  for  $V_D=V_S=0$ .  $C_{gd}$  and  $C_{gs}$  are equal and the value of the gate capacitance  $C_{gg}$  approximates to the oxide capacitance both in accumulation and strong inversion, as it should be.

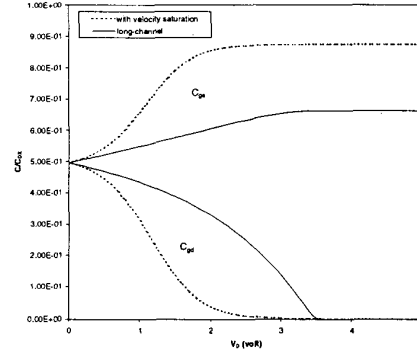


Fig.3 -  $C_{gs}$  and  $C_{gd}$  calculated with velocity saturation included and for the long-channel device (1) versus  $V_D$ , with  $V_G=5V$  and  $V_S=V_B=0V$ .

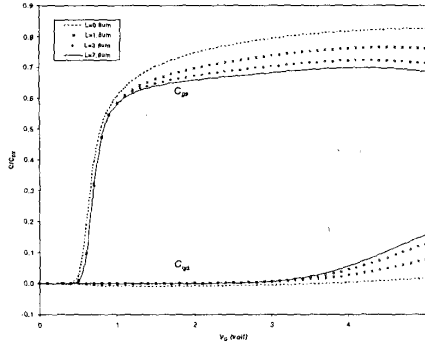


Fig.4 -  $C_{gs}$  and  $C_{gd}$  versus  $V_g$  for channel-lengths varying from  $0.8\mu\text{m}$  to  $7.8\mu\text{m}$ .  $V_g=5\text{V}$  and  $V_s=V_b=0\text{V}$ .

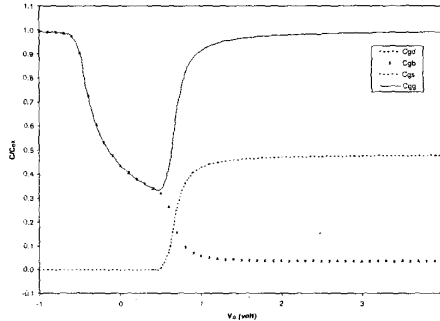


Fig.5 -  $C_{gd}$ ,  $C_{gs}$ ,  $C_{gb}$  and  $C_{gsb}$  versus  $V_g$  for  $V_g=V_s=V_b=0\text{V}$

## 5. Conclusions

A model for charges and (trans)capacitances for the MOS transistor was presented. The model is consistent with the drain current model, and has compact and continuous expressions for the (trans)capacitances. The results of simulations show the consistency of the model.

## Acknowledgements

The authors would like to thank the financial support of CNPq and CAPES, from the Brazilian Ministries of Science and Technology and Education.

## 6. References

- [1] O. C. Gouveia-F., A. I. A. Cunha, M. C. Schneider, and C. Galup-Montoro, "The ACM model for circuit simulation and equations for SMASH", [ONLINE]. Available WWW: <http://www.dolphin.fr>.
- [2] K. Joardar, K. K. Gullapalli, C. C. McAndrew, M. E. Burnham and A. Wild, "An improved MOSFET model for circuit simulation", IEEE Transactions on Electron Devices, vol. 45, pp. 134-148, January 1998
- [3] Y. Cheng, M. Jeng, Z. Liu, J. Huang, M. Chan, K. Chen, P. K. Ko and C. Hu, "A physical and scalable I-V model in BSIM3v3 for analog/digital circuit simulation," IEEE Trans. Electron Devices, vol. 44, n° 2, pp. 277-287, February 1997
- [4] M. A. Maher, "A Charge-Controlled Model for MOS Transistors", Tanner Tools Internal Report, Pasadena, CA, USA, 1989.
- [5] K. Lee, M. Shur, T. A. Fjeldly, and T. Ytterdal, Semiconductor Device Modeling for VLSI, Prentice-Hall, Englewood Cliffs, NJ, 1993.

Table 1.  
Expressions for the (trans)capacitances

Variable	Expression
$C_{gs(d)}$	$C_{gs(d)o} - (C_{gso} + C_{gdo}) \frac{\sigma}{n} + \left( 1 - \frac{q_f^2 + q_r^2}{(q_f + q_r)^2} \right) \frac{L_{cq}}{v_{lim}} g_{ms(d)}$
$C_{gb}$	$\frac{n-1}{n} (C_{ox} - C_{gso} - C_{gdo}) - ((n-1)C_{ox} + C_{gso} + C_{gdo}) \frac{2\sigma}{n} + \frac{2}{3} \left( 1 - \frac{q_f^2 + q_r^2}{(q_f + q_r)^2} \right) \frac{L_{cq}}{nv_{lim}} g_{mb}$
$C_{dd(s)}$	$C_{dd(s)o} + (C_{dst(o)} - C_{dd(s)o}) \frac{\sigma}{n} + \left( \frac{2}{15} \frac{3q_f^3 + 11q_f^2q_r + 14q_fq_r^2 + 2q_r^3}{(q_f + q_r)^3} - \frac{1}{2} \right) \frac{L_{cq}}{v_{lim}} g_{ms(d)}$
$C_{dg}$	$\frac{(C_{ddo} - C_{dso})}{n} - \left( \frac{2}{15} \frac{3q_f^3 + 11q_f^2q_r + 14q_fq_r^2 + 2q_r^3}{(q_f + q_r)^3} - \frac{1}{2} \right) \frac{L_{cq}}{v_{lim}} g_{mg}$
$C_{db}$	$\frac{(C_{ddo} - C_{dso})}{n} (n-1-2\sigma) - \left( \frac{2}{15} \frac{3q_f^3 + 11q_f^2q_r + 14q_fq_r^2 + 2q_r^3}{(q_f + q_r)^3} - \frac{1}{2} \right) \frac{L_{cq}}{v_{lim}} g_{mb}$
$C_{bs(d)}$	$(n-1)C_{gs(d)}$